# Si Micromachining for High-Frequency Applications

Linda P. B. Katehi
Department of Electrical Engineering and Computer Science
The Radiation Laboratory
The University of Michigan,
Ann Arbor, MI 48109
USA

## Abstract

High frequency applications impose very strict requirements on circuit performance including low loss, low dispersion and negligible parasitics. This paper reports on the development of a new family of circuits based on Si micromachining. These circuits exhibit excellent RF properties and have a great potential for high yield and low cost. Their fabrication is based on conventional Si/GaAs/InP fabrication techniques and, as such, they preserve their monolithic character while at the same time allow for high density and three-dimensional integration.

## Introduction

Micromachined high-frequency circuits with integrated packaging offer light weight and controllable parasitics, which makes them appropriate for hand-held communication systems and miniature intelligent millimeter-wave sensors where system requirements impose strict limits on electrical performance. Recent advances in semiconductor processing techniques allow for integration in all of the directions of the three-dimensional space. The capability to incorporate one more dimension, and a few more parameters, in the circuit design, leads to revolutionary shapes and integration schemes. These circuit topologies have reduced ohmic loss and are of free parasitic radiation or parasitic cavity resonances without loosing their monolithic character. Integration capabilities are thereby extended and performance is optimized. The evolution of micromachined circuits and antennas for operation in microwave and millimeter-wave frequencies is still in its infancy. However, presented here is a description of recent accomplishments in this area, with emphasis on the effort performed at the University of Michigan. There are two techniques which have shown promise for use, and which extensively use micromachining to realize novel circuits. The first utilizes dielectric membranes to support transmission line and antenna configurations [1]-[2] and emphasizes optimization of circuit performance. The second technique introduces new concepts in packaging such as adaptive or conformal packaging and, in addition to improvement in performance, it emphasizes size/volume/cost reduction [3]. The merits of each approach, in relation to electrical performance, fabrication, and compatibility, will be presented, and the impact of the newborn technologies to the state of the art will be discussed. In the following sections a variety of micromachining approaches will be described as they apply to both monolithic circuits and antennas.

## Dielectric Membrane Supported Circuits

The successful development of a membrane-supported transmission line, called microshield, was presented for the first time in the 1991 MTT-S International Microwave Symposium [1]. The microshield is only one of the possible membrane-supported geometries shown in Figure 1. All of these geometries are evolutions of conventional planar lines with one major difference; the substrate material underneath the lines has been removed and a membrane is utilized to support the conductors. Figure 1a shows a finite ground coplanar waveguide line, where the material between the conducting planes has been removed to reduce loss and dispersion. Furthermore, the line is shielded to eliminate parasitic radiation. The second of the micromachined geometries, Figure 1b, is the microshield line, very similar in shape with the conventional coplanar waveguide. This line has zero dispersion, limited parasitic radiation and the capability to suppress the excitation of the unwanted slot-line mode due to the presence of the folded ground which operates as a continuous air bridge.

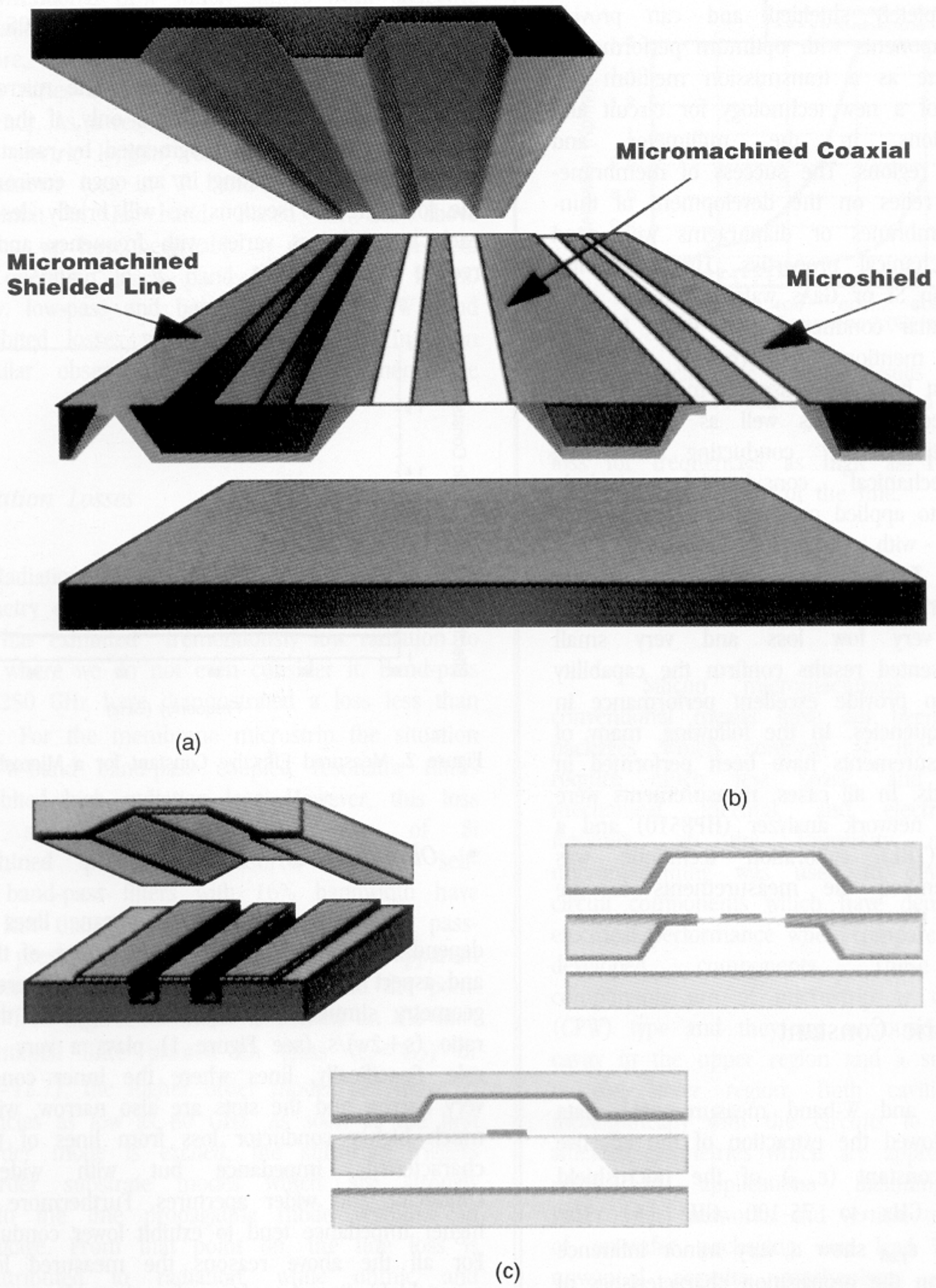

Figure 1. Micromachined Transmission lines (a) Packaged Finite Ground Coplanar Waveguide, (b) Microshield, (c) Packaged Membrane Microstrip

Figure 1c shows a membrane stripline which is characterized by zero dielectric loss, zero dispersion, zero parasitic radiation while maintaining compatibility to planar monolithic geometries. This propagating structure is completely shielded and can provide passive circuit components with optimum performance. The membrane line as a transmission medium has created the basis of a new technology for circuit and antenna applications in the millimeter and submillimeter-wave regions. The success of membrane-supported circuits relies on the development of thin-film dielectric membranes or diaphragms with good electrical and mechanical properties. These thin-film layers are grown on Si or GaAs wafers, and are used to support the planar conducting strip lines. In view of the previously mentioned performance objectives, the thin films must have low losses at microwave and millimeter-wave frequencies, as well as compatibility with semiconducting and conducting materials. Furthermore, mechanical considerations include reduced sensitivity to applied pressure and temperature variations, along with increased membrane or diaphragm sizes. Transmission lines and circuits printed on dielectric membranes have demonstrated zero dispersion, very low loss and very small parasitics. The presented results confirm the capability of these circuits to provide excellent performance in millimeter-wave frequencies. In the following, many of the presented measurements have been performed in the Ka and W bands. In all cases, measurements were made on a vector network analyzer (HP8510) and a Thru-Reflect-Line (TRL) calibration technique was employed to de-embed the measurements to the reference planes of the circuits.

## Effective Dielectric Constant

During Ka and W-band measurements, data were taken that allowed the extraction of the effective relative dielectric constant ($\varepsilon_{r,eff}$) of the microshield line from 10-40 GHz to 75-100 GHz [5]. The measured values of $\varepsilon_{r,eff}$ show a very minor influence of the membrane on the propagation characteristics of the microshield line. The membrane is a 1.5 micron thick tri-layer composite of SiO2/Si3N4/SiO2 with thicknesses of 7000Å/3000Å/4000Å. The dielectric constant of the oxide is 3.9 and of the nitride is 7.5. The presence of the dielectrics results in a value of 1.08, as shown in Figure 2, for $\varepsilon_{r,eff}$, instead of the unity value that would be expected if the signal were propagating entirely in air. Also, very low dispersion is indicated, since the measured $\varepsilon_{r,eff}$ remains very nearly constant vs. frequency. This fact means the absence of substrate moding i.e. single-mode TEM wave propagation over a very wide bandwidth.

## Attenuation in Micromachined Lines

The attenuation in membrane micromachined lines is due to conductor losses only, if the lines are shielded, and it may be augmented by radiation losses if the lines are operating in an open environment. In the following two sections we will briefly describe how each type of loss varies with frequency and ways to reduce or eliminate it.

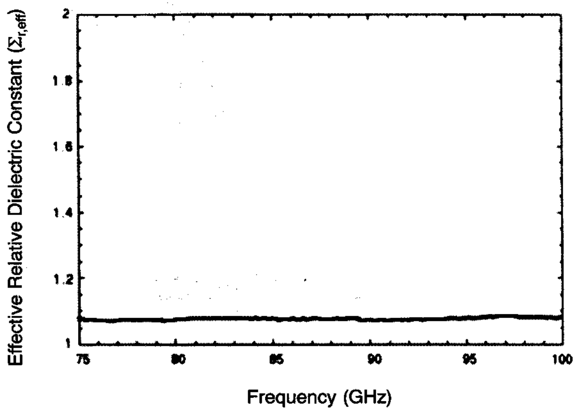

Figure 2. Measured Effective Constant for a Microshield Line.

- *Ohmic Losses*

Conductor loss in membrane lines critically depends on the operating frequency, size of the circuit and aspect ratio. For a microshield line where the line geometry simulates a coplanar waveguide, the aspect ratio (s+2w)/s (see Figure 1) plays a very important role. Specifically, lines where the inner conductor is very narrow and the slots are also narrow, will have a much higher conductor loss from lines of the same characteristic impedance but with wider inner conductor and wider apertures. Furthermore, lines of higher impedance tend to exhibit lower conductor loss. For all the above reasons the measured loss of a microshield line has been found to be much lower than the loss of a coplanar waveguide of the same aspect ratio. On wafer and electro-optic sampling measurements performed at Michigan has demonstrated the low loss characteristics of the microshield line. Measured loss shows that the microshield attenuation constant in dBs/mm is three times lower than that of the conventional coplanar waveguide for frequencies up to 40 GHz. These measurements have shown that losses in these membranes lines remain extremely low as we cross

100GHz and move toward 1000GHz operating frequencies, (see Figure 3).This is due to the fact that the membrane line has only conductor loss contrary to the conventional CPW which suffers from dielectric and radiation loss in addition to ohmic loss. Furthermore, the conductor loss in dB per guided wavelength varies as the inverse of the square root of the frequency. As a result, circuits which are scaled so that their electric lengths remain the same will have lower conductor loss in W band from the loss they would exhibit in Ka band. Based on the above observations, we have been able to design microshield lines for operation in W band with very low losses. Specifically, low-pass and band-pass filters in W band have exhibited losses with less than 1 dB insertion loss. Similar observations apply to the membrane microstrip.

- *Radiation Losses*

Radiation losses have a different frequency and geometry dependence. The membrane microshield geometry has exhibited tremendously low radiation to the point where we do not even consider it. Band-pass filters at 250 GHz have demonstrated a loss less than 1 dB [7]. For the membrane microstrip the situation changes. W-band band-pass coupled resonator filters have exhibited high radiation loss. However, this loss can be suppressed through the use of Si micromachined packages. Measured W-band self-packaged band-pass filters with 16% bandwidth have exhibited less than 0.6 dB loss throughout the pass-band. The presence of radiation loss becomes apparent as the operating frequency increases beyond the point where the first high-order mode is excited on the line. In conventional lines printed on glass ($\varepsilon_r=4.5$) or GaAs ($\varepsilon_r=12.7$), the higher order modes are triggered at frequencies as low as 80 GHz. As soon as the first higher order mode is excited, the substrate triggers higher order substrate modes which are strongly coupled to the line propagating mode resulting in power leakage. From that point on, the line loss is mostly attributed to radiation, while ohmic and dielectric loss play a secondary role.

This well understood fact has been observed experimentally through electro-optic sampling measurements [6]. Figure 3, shows the measured loss factor for three coplanar waveguide lines printed on GaAs, Fused Silica and Si Membrane indicating excessive losses in GaAs for frequencies exceeding 300 GHz. Fused silica behaves well up to 500 GHz but its performance breaks down at around 700GHz. The micromachined coplanar waveguide exhibits minimal loss for frequencies as high as 1THz reflecting the excellent performance of the line.

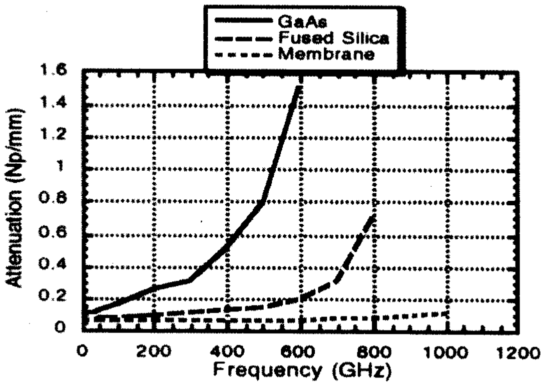

Figure 3. Electro-optic Sampling Results for Coplanar Waveguide Lines Printed on GaAs, Fused Si and GaAs

## On-Wafer Packaged Components

Silicon micromachining can offer what conventional means have not been able to provide; packages which conform to the circuit geometry, require much less space, and provide superior mechanical, thermal, and electrical performance. Recently, at the University of Michigan, Si micromachining was used to develop self-packaged circuit components which have demonstrated superior electrical performance when compared to conventionally developed components. These micromachined components are of microstrip or coplanar waveguide (CPW) type and they are surrounded by an air-filled cavity in the upper region and a substrate-filled cavity in the lower region. Both cavities are integrated monolithically with the circuits to provide completely shielded geometries which are appropriate for a broad range of applications including high density interconnect networks and vertical transitions. The use of on-wafer packaging can lead to elimination of unwanted parasitic mechanisms such as parasitic coupling and parasitic radiation.

As discussed earlier, Si micromachining allows for an on-wafer packaging without affecting the integration capability. To illustrate the effect of a micromachined conformal package in the reduction of cross-talk, a back-to-back right angle bend is designed in an open as well as packaged configuration (Figure 4). The conventional microstrip environment is referred to as "open" while the shielded one is referred to as "packaged".

In this work, the circuits and upper cavities are developed on high and low resistivity silicon substrates, respectively, with a thickness of 500 μm. In the packaged circuits the wafer has been thinned locally under the transmission line to 320 μm to provide better propagating conditions (quasi-TEM propagation). Both open and packaged circuits incorporate 50 ohm lines. In the packaged configuration, the bottom wafer supports the planar circuits and lower cavity of the package while the top wafer has the upper cavities (Figure 4).

Ground pads have been incorporated on the same plane as the conducting lines for bonding between the upper and lower cavities. These planes are located 380 μm away from the conducting line to ensure a microstrip mode of propagation.

For the back-to-back right angle bend, the conformal package is developed using the techniques described in [3]. There are two distinct fabrication issues addressed in this work. First, reduction of wafer thickness under the conducting lines and second, the realization of convex corners around the bends in the upper and lower cavity regions. To locally reduce the thickness of the wafer from 500 to 320 μm and provide the necessary DC contact areas, a two step etch procedure was employed. Initially the outer channels of the lower package were removed while the center feedline channel is protected with silicon dioxide. Next, the oxide masking layer is removed and the wafer is etched an additional 170 μm to locally reduce the center regions to 320 microns (See Figure 5). Convex corner undercutting is compensated by including centered squares at the edge of each convex corner [4]. The compensation squares are approximately 1.4 times the desired etch depth. Such a correction has been incorporated in the designs for the upper and lower wafers.

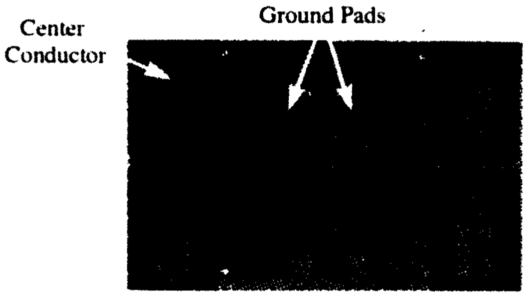

(A) BACK-TO-BACK RIGHT ANGLE BENDS

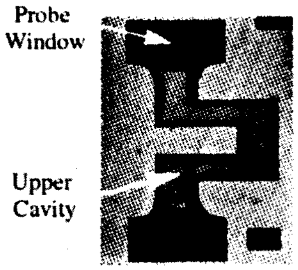

(B) MICROMACHINED PACKAGE

Figure 4. On-Wafer Packaged Microstrip Bonds

(a) Cross-Section of Micromachined Package

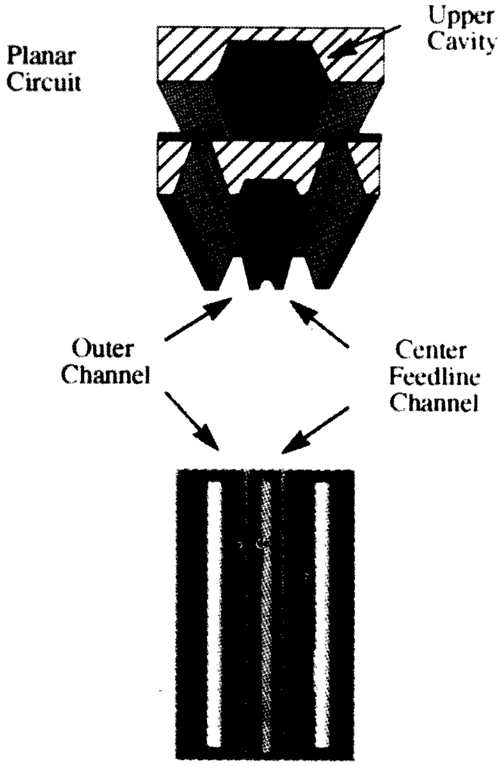

(b) Photograph of Bottom of Lower Cavity Wafer

Figure 5. (a) Illustration of the Package Cross Section with Localized Substrate Region for the Conducting Line, (b) Photograph of the Lower Side of the Package

Measured data are discussed regarding coupling of the planar bend geometries. The coupling of the planar bend geometry to nearby elements is characterized with on-wafer probing. A Short-Open-Load-Thru calibration method is employed using 150 μm pitch Picoprobes from GGB Industries with an 8510C Network Analyzer and Alessi Probe station. Cross-coupling effects are determined by measuring the input of the bend structure and the output of a neighboring element adjacent to the bend geometry. environments is compared in Figure 6. In the lower frequency range the difference in the insertion loss is due to ohmic losses in the cavities of the packaged bend. In Figure 6, the open structure has coupling as high as -20 dB in the 5 to 30 GHz range. Similar measurements have been performed on the packaged structure. The results demonstrate coupling less than -

45 dB which is very close to the coupling between the two probes when left out of contact in air.

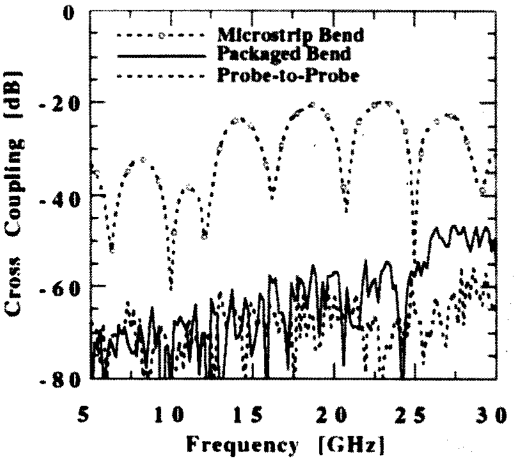

Figure 6. Coupling Between two Open and two Packaged Lines as Compared to the Coupling Between two Probes Left Open

To illustrate this packaging approach in an antenna application, a package surrounding the feeding line of a micro-strip patch antenna has been incorporated in the design (See Figure 7). In this circuit, only the substrate under the feeding line has been thinned to ensure clean propagation of a dominate microstrip mode. The substrate under the antenna has been left at its original thickness but dielectric material has been removed locally to provide higher antenna efficiency. In Figure 8, the performance of the open and packaged design is shown which illustrates that the package provides the appropriate shielding while maintaining the desired strength of the patch resonance. As observed from the measurements, the bandwidth of the packaged antenna is higher than the bandwidth of the open antenna by 110% (VSWR≤1.8). This increase indicates higher antenna efficiency and is attributed to the fact that the propagation characteristics (b, Zo) in the package feedline are less sensitive to the frequency due to the improved TEM propagation on the line and the effective dielectric constant under the antenna is substantially reduced due to the removed material. Therefore, the resulting package can be easily extended to array applications where feedline radiation can be eliminated.

## Micromachined Components

The performance advantages of membrane supported transmission lines can be clearly demonstrated by observing the characteristics of various distributed circuits which are common to planar microwave circuitry and MMICs. The broadband TEM propagation afforded by membrane supported transmission lines permits a significant increase in performance levels for typical planar circuits such as filters, stubs, and power dividers. As an example of a micromachined component let us consider a low-pass filter with cut-off frequency at 22GHz. This filter is made as a combination of distributed components, stubs, and lumped elements, MIM capacitors, carefully placed on the stubs in between the coupling lines (see Figure 9). The filter is printed on a thin Si membrane and is excited from two probe pads located on the silicon substrate. This filter represents a new approach to component design where distributed and lumped elements are combined appropriately to improve electrical performance. In this particular filter, the resonating stubs have been utilized to provide the low-pass character, while the capacitors have been placed to compensate for inductive parasitics, reduce the required size and also suppress the parasitic pass bands which normally occur at $2f_c$, $3f_c$ etc. Pictures of the front and back of capacitors and the Si cavities are shown in Figures 9a and 9b. Furthermore, theoretical and experimental results for this filter are shown in Figure 9c and indicate excellent agreement. These results confirm the very low loss characteristics of the lines and demonstrate the capability of effectively suppressing the parasitic pass-bands to below -40 dB at frequencies as high as $5f_c$ [7].

## Conclusions

A new micromachined technology suitable for three-dimensional planar circuit configurations has been presented. At higher frequencies, problems associated with the substrates make conventional approaches unfeasible, and membrane supported circuit components offer the only planar alternative to costly waveguide-based approaches. Micromachined transmission lines and circuits have been shown to perform very well in frequency bands all the way up to W-band (110 GHz). Circuits commonly used in CPW implementations are shown to have superior performance when realized with membrane supported transmission lines like the microshield line. The microshield line has a relative effective dielectric constant of 1.07 through 100 GHz and, as a result, it exhibits zero dispersion and zero substrate loss. The micromachined CPW has the lowest attenuation yet demonstrated for planar transmission lines. Filters and resonant stubs have been measured up to 250 GHz and have demonstrated an unparalleled electrical performance. Micromachining has also opened the doors to techniques for fabricating circuits that were previously restricted by cumbersome machining processes. Interdigitated filters were thought to be limited to very low frequencies where they could be manufactured using mechanical techniques, but membrane technology has allowed them to become high performance alternatives at 30 GHz. Membrane millimeter-wave microstrip inductors have been developed and fabricated on a high-resistivity silicon substrates using micro-machining techniques with resonant frequencies in the submillimeter-wave region. Last but not least, on-wafer packaging can eliminate parasitic coupling and radiation by component-specific electromagnetic shielding without disturbing the monolithic character of the circuit.

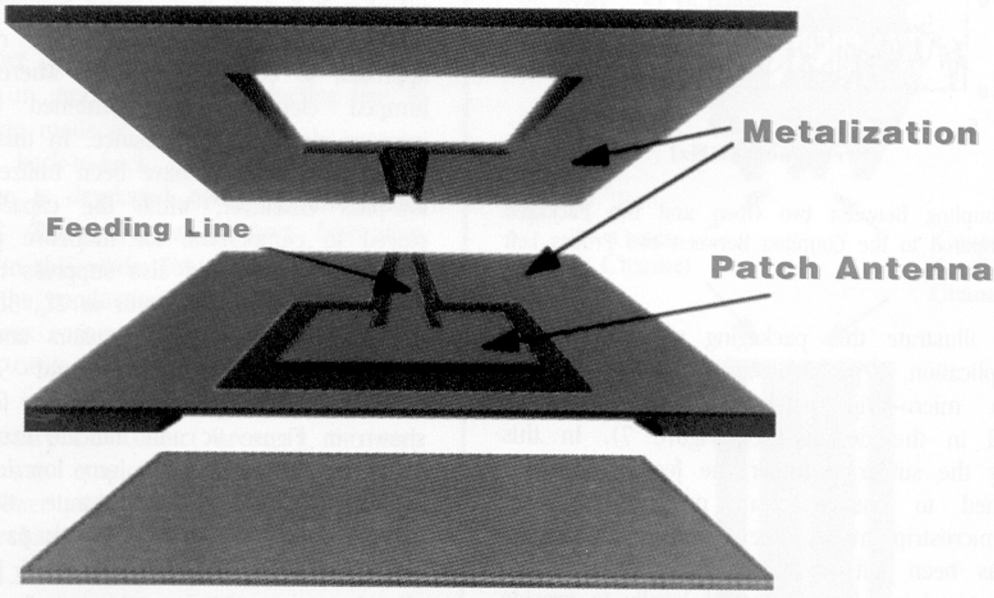

Figure 7. Micromachined Antenna

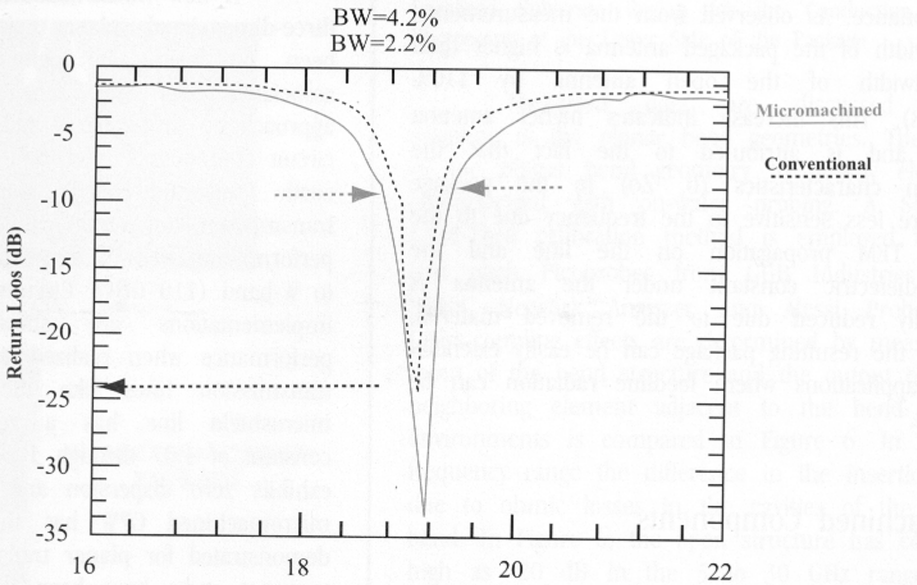

Figure 8. Input Match

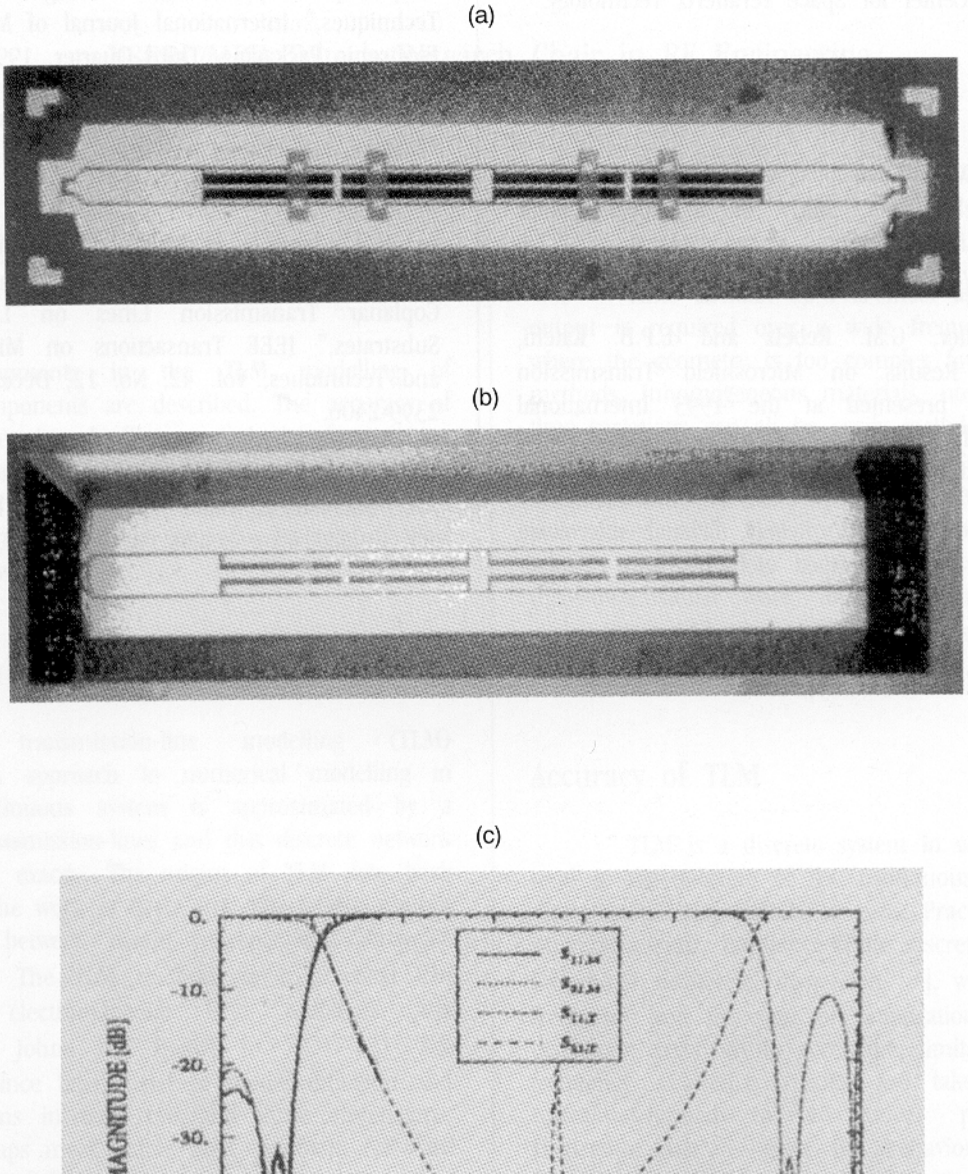

Figure 9. Micromachined Membrane Low-Pass Filter: (a) Front View, (b) Back View, (c) Theoretical and Experimental Results

## Acknowledgments

This work was performed at The University of Michigan and has been supported by contracts from the Army Research Office, the Office of Naval Research and the NASA Center for Space Terahertz Technology.

## References

[1] N.I. Dib, W.P. Harokopus, L.P.B. Katehi, C.C. Ling and G.M. Rebeiz, "A Study of a Novel Planar Transmission Line," presented at the 1991 IEEE MTT-S International Symposium, Boston, MA, June 1991.

[2] T.M. Weller, G.M. Rebeiz and L.P.B. Katehi, "Experimental Results on Microshield Transmission Line Circuits," presented at the 1993 International Symposium of the IEEE Microwave Theory and Techniques Society, Atlanta, Georgia, June 1993.

[3] C. Y. Chi and G. M. Rebeiz, "Planar microwave and millimeter- wave lumped elements and coupled-line filters using micro-machining techniques," IEEE Trans. Microwave Theory Tech., December, 1994.

[4] R. F. Drayton, T. M. Weller, and L. P. Katehi, "Development of Miniaturized Circuits for High-Frequency Applications using Micromachining Techniques," International Journal of Microcircuits and Electronic Packaging, Third Quarter, 1995.

[5] S.V. Robertson, L.P.B. Katehi, and G.M. Rebeiz, "W-Band Microshield Low-Pass Filters," in 1994 IEEE MTT-S Digest, pp. 625-628.

[6] H.-J. Cheng, J. F. Whitaker, T. M. Weller and L. P. B. Katehi, "Terahertz-Bandwidth Characteristics of Coplanar Transmission Lines on Low Permittivity Substrates," IEEE Transactions on Microwave Theory and Techniques, Vol. 42, No. 12, December 1994, pp. 2399-2406.

[7] T.M. Weller, L.P.B. Katehi and G.M. Rebeiz, "A 250 GHz Microshield Band Pass Filter," IEEE Microwave and Guided Wave Letters, Vol. 5, No. 5, pp. 153-156.